Temperature dependent dielectric and magnetic properties of GdFe1xNixO3 (0.0x0.3) orthoferrites

Pawanpreet Kaur, K. K. Sharma, Rabia Pandit, Ravi Kumar, R. K. Kotnala, and Jyoti Shah

Citation: Journal of Applied Physics **115**, 224102 (2014); doi: 10.1063/1.4882115
View online: http://dx.doi.org/10.1063/1.4882115
View Table of Contents: http://scitation.aip.org/content/aip/journal/jap/115/22?ver=pdfcov
Published by the AIP Publishing

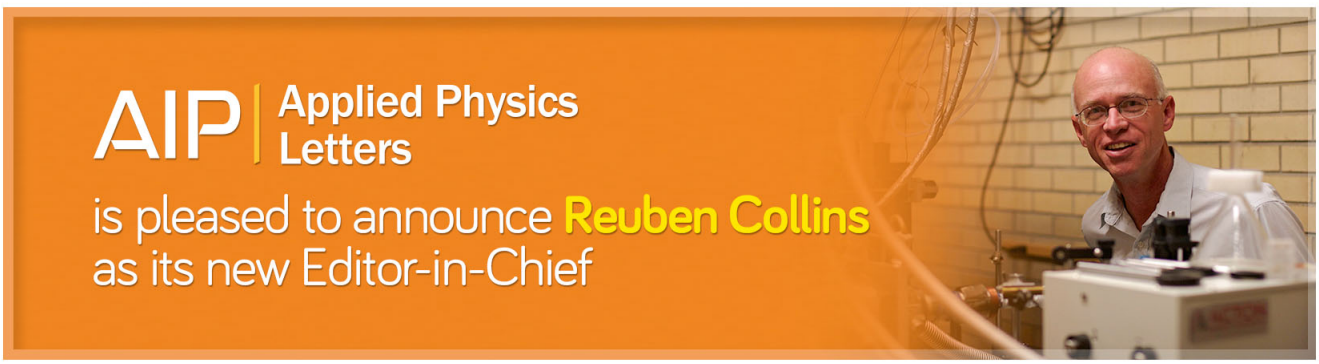

Temperature dependent dielectric and magnetic properties of $GdFe_{1-x}Ni_xO_3$ ($0.0 \le x \le 0.3$) orthoferrites

Pawanpreet Kaur,[1,a)] K. K. Sharma,[1,b)] Rabia Pandit,[1] Ravi Kumar,[2,c)] R. K. Kotnala,[3] and Jyoti Shah[3]
[1]*Department of Physics, National Institute of Technology, Himachal Pradesh, Hamirpur 177005, India*
[2]*Centre for Material Science and Engineering, National Institute of Technology, Himachal Pradesh, Hamirpur 177005, India*
[3]*National Physical Laboratory, New Delhi 110012, India*

(Received 10 March 2014; accepted 27 May 2014; published online 9 June 2014)

The polycrystalline samples of $GdFe_{1-x}Ni_xO_3$ ($x = 0.0, 0.1, 0.2, 0.3$) orthoferrites are synthesized via solid state reaction route. The Rietveld fitted X-ray diffraction patterns confirm the formation of orthorhombic phase with Pbnm space group for all the samples. The dielectric measurements reveal an enhancement in dielectric constant and tangent loss with increase in both temperature as well as Nickel (Ni) substitution. Dielectric studies are also in support with the induction of delocalized charge carriers in the $GdFeO_3$ matrix with increasing Ni doping. Magnetization versus applied field study shows the non-saturating hysteresis curves suggesting the canted type antiferromagnetic behavior in the considered orthoferrites. Moreover, the observed magnetic behavior is complex and the doping affects the magnitude of magnetization differently at 300 K and 80 K. It has further been noticed that the incorporated Ni^{3+} ions enhances the symmetry of the magnetization curves. The as-prepared samples may find their applications in the decoupling capacitors. © *2014 AIP Publishing LLC*. [http://dx.doi.org/10.1063/1.4882115]

INTRODUCTION

The perovskite based ceramic oxides (ABO_3) have been the focus of scientific activity since the last many decades owing to their simple structure, interesting magnetic, transport and optical properties.[1–3] The perovskite structure is amenable to various type dopants, which play a crucial role in tuning its properties. In general formula ABO_3, where A refers to rare earth ion and B to transition metal (TM) ion. Previous studies revealed that B ion plays a key role in controlling electronic and magnetic properties of perovskites. Replacing B ion with Fe^{3+} ion gives rise to orthoferrite family. Rare earth orthoferrites ($RFeO_3$) were first identified by Forestier and Guillian in 1950.[4] $RFeO_3$ exhibits thought provoking magnetic properties like non-collinear antiferromagnetism, high pressure induced spin cross over in iron system.[5,6] They have also been a subject of technological concern because of their applications in magneto-optic devices and in gas sensors.[7,8]

Among orthoferrites, Gadolinium orthoferrite ($GdFeO_3$) seeked much attention as most of the ABO_3 type compounds exhibit crystal structure similar to $GdFeO_3$ and it also displays a rich assortment of interesting magnetic properties. The crystallographic measurements on $GdFeO_3$ were performed by Geller at bell telephonic laboratories, which shows that it crystallizes in an orthorhombic structure with Pbnm space group containing pseudo cubic sub-cells, where Gd^{3+} and Fe^{3+} ions resides at pseudo cube corners and body centers, respectively.[9] Below 660 K, the Fe^{3+} ions are antiferromagnetically ordered along the orthorhombic "a" axis but are slightly canted to give weak ferromagnetism along the orthorhombic "c" axis. The slight canting of Fe^{3+} spins due to anti-symmetric exchange produces a resultant weak ferromagnetism.[5,10] This type of material is important for opto-magnetic devices and memory based devices. Orthoferrites recently also showed the potential as a spintronic material by substituting Ni^{3+} ions at Fe sites.[11–13] But less attention has been paid to the dielectric properties of these materials, as higher dielectric constant materials can be used in capacitive components. So, the purpose of the present work is to gain a deeper insight into the temperature dependent dielectric and magnetic properties of $GdFe_{1-x}Ni_xO_3$ ($0.0 \le x \le 0.3$). This study also helps us to understand the intriguing properties of $GdFeO_3$.

EXPERIMENTAL

Polycrystalline $GdFe_{1-x}Ni_xO_3$ ($0.0 \le x \le 0.3$) samples were synthesized by conventional double sintering ceramic technique. The elementary reagents, Gd_2O_3, Fe_2O_3, NiO of high purity (>99.99%) obtained from Sigma Aldrich, were weighed and mixed in a stoichiometric amount to get the desired compositions. All the samples were calcined at 1000 °C for 12 h, after calcination samples were again ground in a wet medium with acetone to ensure good mixing. Then, the ceramic powders were pressed into required shape by applying a pressure up to 5 tons. It also ensures large areas of surface contact between grains. Finally the samples were sintered twice at 1300 °C for 24 h. To ensure the single phase formation of all the samples, room temperature x-ray diffraction (XRD) was performed by X'pert Pro Panalytical, x-ray diffractometer with Cu K_α radiation in the scanning range $20° \le 2\theta \le 80°$. After ensuring the phase purity of all

a)merry2286@gmail.com
b)kknitham@gmail.com
c)Present address: Beant College of Engineering and Technology, Punjab, Gurdaspur 143521, India.

the samples, the dielectric measurements were carried out as a function of temperature (100 to 300 K) and frequency (75 kHz–5 MHz) using an Agilent 4284 A precision LCR meter. The magnetization measurements were performed using vibrating sample magnetometer Lakshore (7403), USA at 80 K and EZ9 Microsense vibrating sample magnetometer at 300 K.

RESULTS AND DISCUSSION

Rietveld refined XRD patterns of $GdFe_{1-x}Ni_xO_3$ ($x = 0.0, 0.1, 0.2, 0.3$) samples have been shown in Fig. 1. XRD data of all the samples were refined with FullProf suite software version (1.00) February 2007 JGP-JRC using pseudo-Voigt profile function using Pbnm space group, which confirms that the synthesized compounds crystallize in orthorhombic phase.[14] The Rietveld refinement factors, i.e., lattice constant, unit cell volume and goodness of fit (χ^2) for all the samples are tabulated in Table I. Quite satisfactory values of χ^2 have been obtained for all the compositions confirming a good fit between the observed and Rietveld fitted data. The shift in most intense peak position (112) towards higher angle side with increasing Ni^{3+} ions concentration can also be observed from Fig. 1. It confirms that the unit cell volume decreases with increasing nickel substitution, which is attributed to the smaller ionic radii of Ni^{3+} ions (0.56 Å) as compared to Fe^{3+} (0.64 Å) ions.[15]

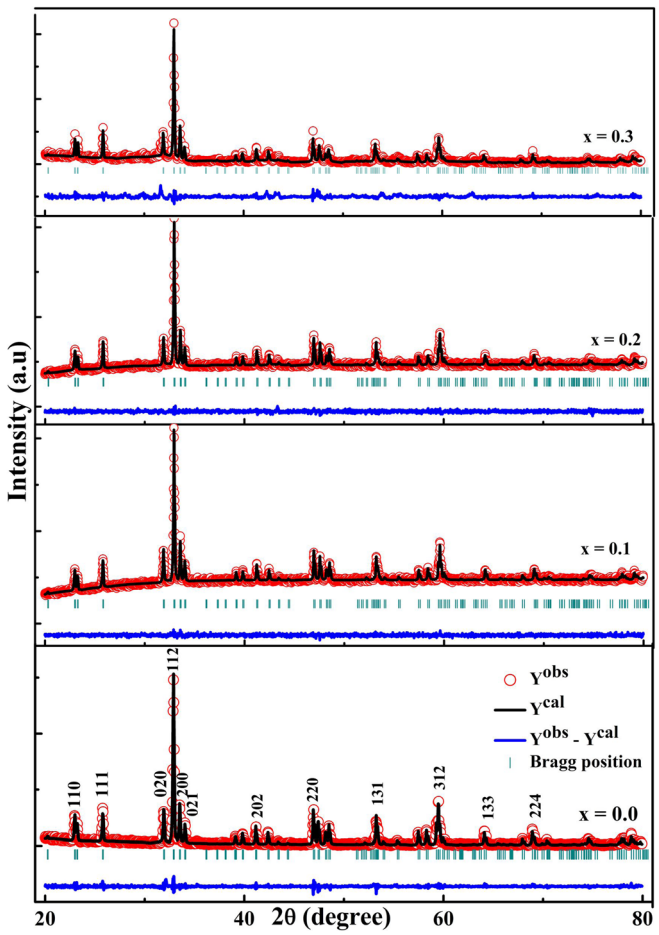

FIG. 1. Rietveld fitted XRD pattern for $GdFe_{1-x}Ni_xO_3$ ($x = 0.0, 0.1, 0.2, 0.3$).

TABLE I. Lattice parameter (a, b, c), unit cell volume (V), and goodness of fit (χ^2) for $GdFe_{1-x}Ni_xO_3$ ($0.0 \le x \le 0.3$) compositions obtained by Rietveld fitting.

x	a (Å)	b (Å)	c (Å)	V(Å)^3	χ^2
0.0	5.3456	5.6058	7.6627	229.6238	1.29
0.1	5.3384	5.6116	7.6427	228.9506	1.20
0.2	5.3359	5.6110	7.6371	228.6531	1.26
0.3	5.3331	5.6089	7.6346	228.3720	1.65

Fig. 2 shows the variation of dielectric constant (ε') as a function of frequency (75 kHz–5 MHz) at different temperatures for $GdFe_{1-x}Ni_xO_3$ ($x = 0.0, 0.1, 0.2, 0.3$). The dielectric constant (ε') is calculated using the formula

$$\varepsilon' = \frac{Ct}{\varepsilon_0 A}, \tag{1}$$

where C, t, A, ε_0 are capacitance, thickness, area, and absolute permittivity of free space, respectively. In the measured temperature and frequency range, ε' decreases with increase in frequency, while increase with increase in temperature for all the compositions. The usual dispersion behavior, i.e., a continuous decrease in ε' at low frequencies, while remaining almost constant at higher frequencies frequency can be attributed to Maxwell–Wagner polarization in agreement with the Koop's phenomenological theory.[16,17] This decrease in ε' and remaining almost constant at high frequencies is due to the fact that beyond a certain frequency, the hooping of charge carriers cannot follow the alternating field and start lagging behind the applied field. Pure composition possesses high dielectric constant even at room temperature, which is consistent with the dielectric reports of other orthoferrites.[18,19] This is due to the close-packing of oxygen ions having loosely bound electrons, as these electrons get distorted in an applied electric field.[19]

On comparing the compositional variation of ε', it can be noticed that the magnitude of the dielectric constant as well as dispersion has increased in the $x = 0.1, 0.2, 0.3$ samples as compared to the pure sample. The observed enhancement in dielectric constant may be due to the fact that Ni^{3+} ions doping induces free charge carriers in the system, hence the high polarisibility of conductive particles can be responsible for the increase in dielectric constant.[20]

The observed increase in ε' at higher temperatures for all compositions can be attributed to the fact that the charge hopping is a thermally activated process hence polarization enhances with increasing temperature.[21] Fig. 3 shows the temperature dependence of dielectric constant at the selected frequencies, it can be inferred that the rate of increase of dielectric constant varies in different temperature regimes. The slow increase in ε' below the critical temperature (T_c) can be attributed to the fact that, thermal energy given to the samples was not enough to free the localized dipoles to be oriented in the field direction. Whereas above T_c increased temperature liberates more localized dipoles, which then get aligned in the field direction.[22] The decrease in critical temperature is noticed from approximately 200 °C for $x = 0.0$ to 160 °C for $x = 0.3$. It has further been noticed from the Fig. 3

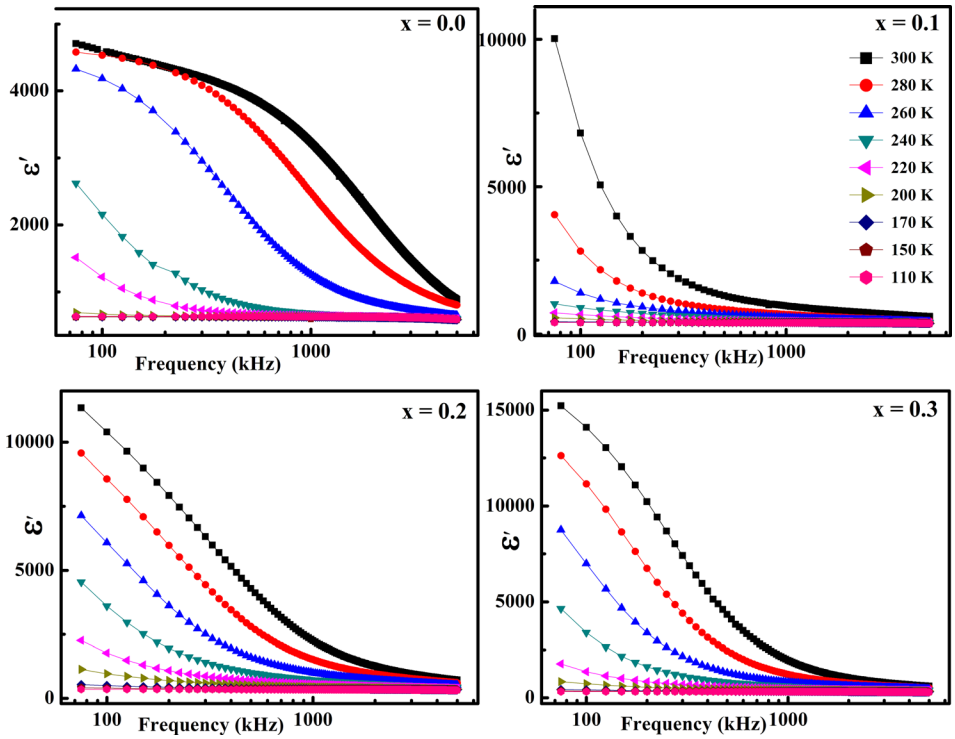

FIG. 2. Dielectric constant as a function of frequency at different temperatures.

that below 170 K dielectric constant of doped samples has lesser value than that of pure. However, at room temperature their ε' attains greater value as compared to the x = 0.0 sample, implying to the enhanced contribution of delocalized charge carriers above 170 K.

The temperature dependence of tangent loss (tan δ) as a function of frequency for all the compositions has been plotted in Fig. 4. Dielectric loss arises due to lag of polarization behind the applied alternating electric field. It is evident that the loss increases with increase in temperature and also the loss peak shift towards higher frequency with increase in the temperature for all compositions. The observed peaks reflect a strong correlation among the conduction mechanism and dielectric behavior.[22] The peak in

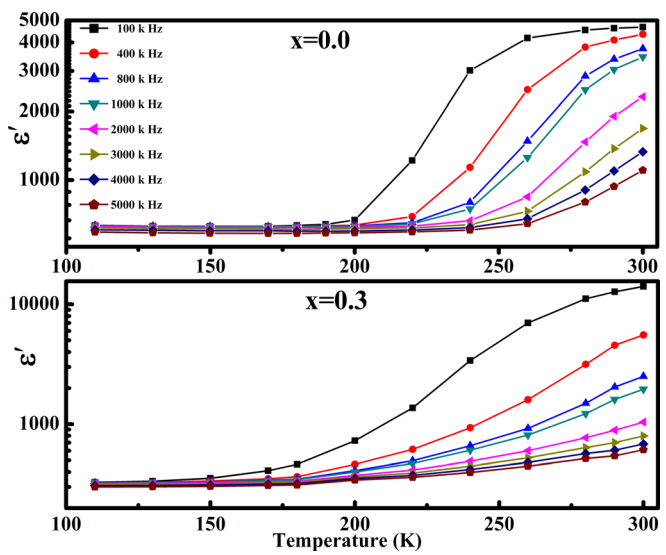

FIG. 3. Dielectric constant as a function of temperature for x = 0.0, 0.3 at different frequencies.

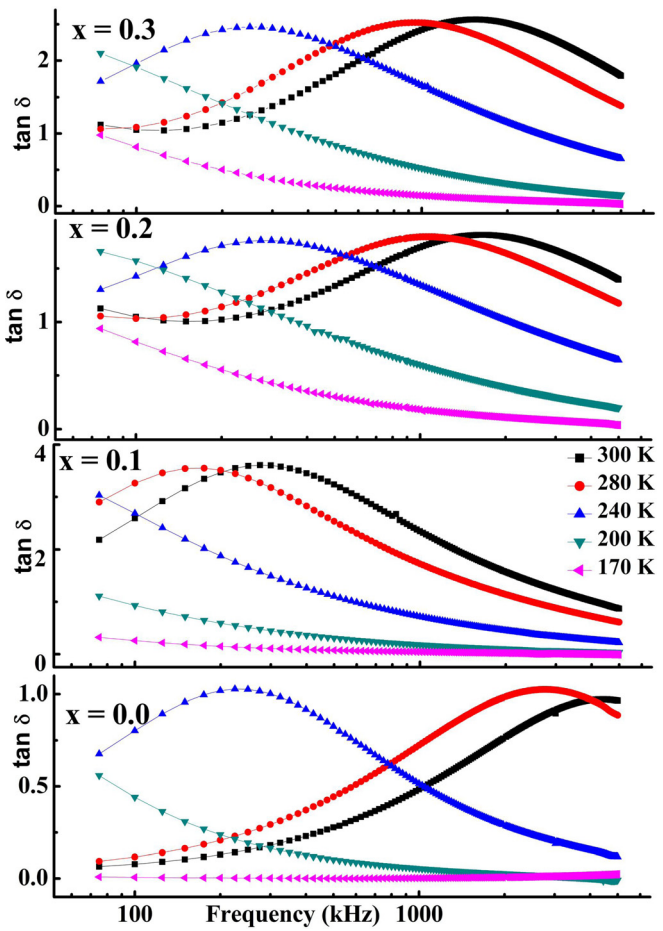

FIG. 4. Tangent loss as a function of frequency at various temperatures.

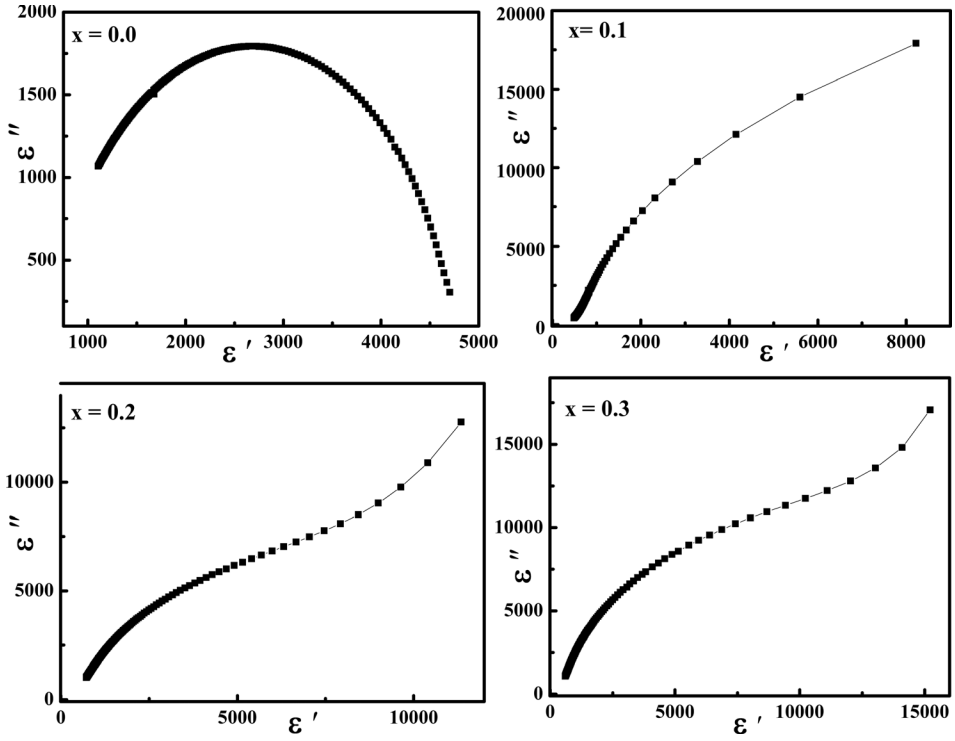

FIG. 5. Cole-Cole plots for all compositions at 300 K.

the loss factor can be attributed to the Maxwell–Wagner interfacial polarization, where the matching of hopping frequency with the frequency of an applied field. On the other hand, it can also be perceived from the Fig. 4 that tangent loss has higher value for Ni doped samples as compared undoped, supporting to the enhanced free charge motion within the doped compositions at higher temperatures. The loss peaks in Ni^{3+} doped samples (x = 0.1, 0.2, 0.3) are comprehensive to more dispersion in their dielectric constant. The loss peak is not comprehensible for x = 0.0, at room temperature as it may occur beyond the studied range of frequency, i.e., 5 MHz.

For the knowledge of distribution of relaxation times the Cole–Cole plots are drawn between ε'' (f) versus ε' (f) at room temperature, in Fig. 5. The plots do not fit into complete semicircles indicating non—Debye type relaxation phenomena in these materials. It is clear that the Ni^{3+} ion substitution has a significant effect on the shape of Cole–Cole plots. According to the Grant both large values of conductivity or high-frequency capacitance are the possible reasons for losing semicircle shape of the Cole-Cole plot and it start behaving like an asymptotic curve.[23]

The dielectric data have also been presented in the form of the complex dielectric modulus $M^*(\omega)$ form to avoid the effects of electrode and contact conductivity. The dielectric modulus is an electrical analogue to the dynamic mechanical shear modulus and is inversely related to the complex permittivity.[24] The dielectric modulus is represented as

$$M^*(\omega) = \frac{1}{\varepsilon^*(\omega)} = M'(\omega) + iM''(\omega). \quad (2)$$

The real (M′) and imaginary (M″) parts of the complex electrical modulus were obtained using the relation

$$M' = \frac{\varepsilon'(\omega)}{\varepsilon'(\omega)^2 + \varepsilon''(\omega)^2} \quad \text{and} \quad M'' = \frac{\varepsilon''(\omega)}{\varepsilon'(\omega)^2 + \varepsilon''(\omega)^2}, \quad (3)$$

where obtained ε' and ε'' represent the real and imaginary parts of dielectric constant. The variation of M" as a function of frequency at different temperatures has been shown in Fig. 6. The data thus presented exhibit a clear peaking behavior at the conductivity relaxation frequency (f_m) for the typical temperatures. It is clearly evident that the relaxation hump gradually shifts towards the high frequency side with the increase in temperature, implying the decrease in relaxation time (τ) or an increase in conductivity. It is observed that the relaxation time for x = 0.0 sample decreases from $5.30 \times 10^{-1}\,\mu s$ to $6.14 \times 10^{-2}\,\mu s$ as temperature increases from 220 to 260 K.

Furthermore, the effects of Ni^{3+} ions substitution in $GdFeO_3$ crystal lattice can be noticed clearly from the peaking behavior observed at different temperatures in all the samples (see Fig. 6). The relaxation frequency is shifting towards the high frequency side at all the measured temperatures with increase in Ni doping. The relaxation time decreases from to $5.3 \times 10^{-1}\,\mu s$ to $1.13 \times 10^{-1}\,\mu s$ as the Ni concentration increases from x = 0.0 to 0.3, respectively, at 220 K. The lower value of τ for the doped samples supports the increase in conductivity for the same. The peak does not appear for some temperatures for different compositions, this may be due to the insufficient temperature or the peaks may be occurring below/upper the range of frequency of the instrument used.

The temperature dependence of conductivity relaxation frequency (f_m) as a function of temperature can be expressed as

$$f_m = f_0 \exp\left(\frac{-E_a}{k_B T}\right), \quad (4)$$

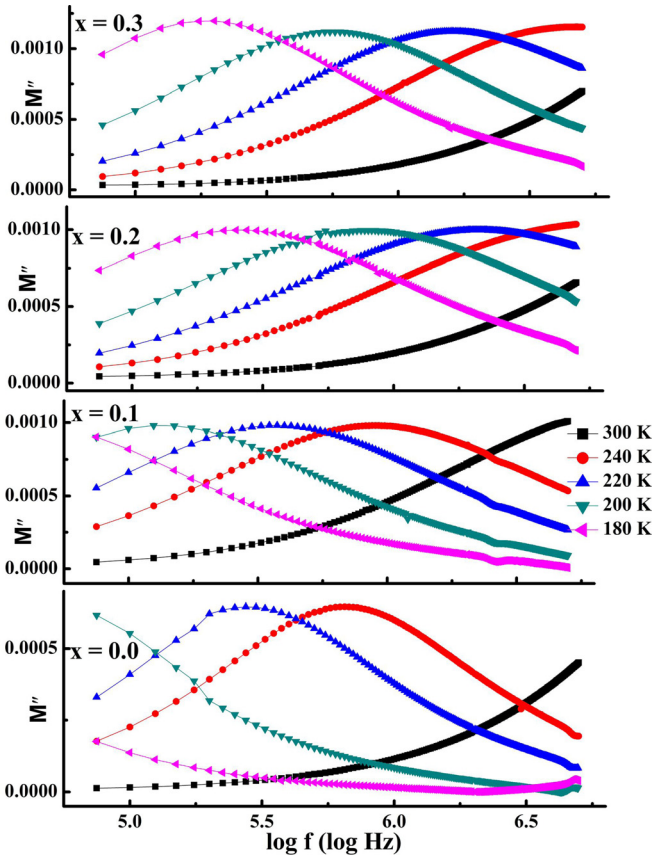

FIG. 6. M″ as function of frequency at different temperatures.

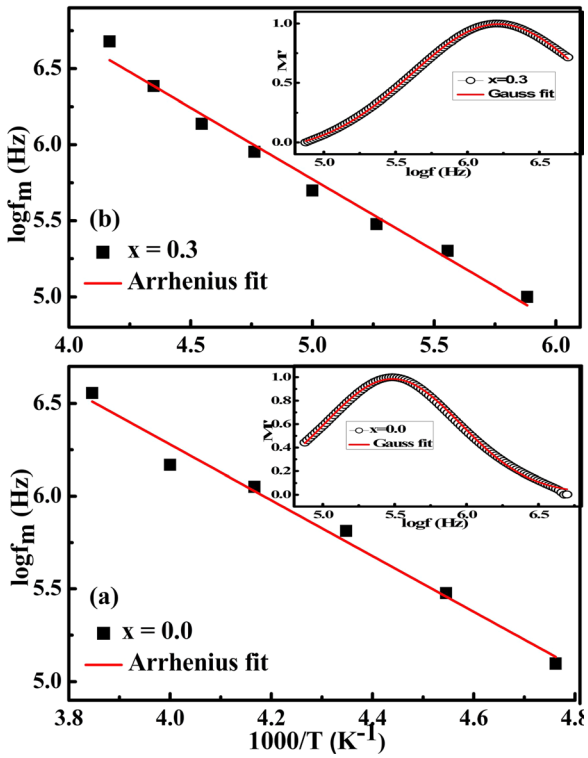

FIG. 7. Plot of peak position extracted from M″ peak at different temperatures as a function of 1000/T (a) for x = 0.0 (b) x = 0.3. Inset shows gauss fit to the normalized M″ versus frequency graph.

where f_0, E_a, k_B, T are the pre-exponential factor, activation energy, the Boltzmann constant, and temperature, respectively. The calculated values of the activation energy (E_a) from the slope of the linear fit (see Fig. 7) reveals that E_a decreases from 0.13 eV to 0.08 eV as Ni ions concentration increases from x = 0.0 to x = 0.3, which in turn contributes to the enhancement of conductivity in doped sample. Furthermore, the values of the stretched exponent (β) estimated from the full width at half maxima (w) of the normalized M″ (ω) vs frequency graph gives an idea about the type of relaxation present in a system (Debye or non-Debye). For $\beta = 1$, the system exhibits Debye relaxation and if $\beta < 1$, it exhibits non-Debye relaxation, where $\beta = 1.14/w$.[25] In the considered samples β value varies from 0.9 to 0.7 which is less than 1, indicating the presence of non-Debye type relaxation behavior in these materials (see inset of Fig. 7).

Orthoferrites display antiferromagnetic (AF) order below the Curie temperature depending on the atomic size of rare earth involved.[26] For most of orthoferrites, the weak ferromagnetism is due to the low symmetry of the magnetic unit cell producing canted structure in Fe sub-lattice. Hence, for a better understanding of such magnetic behavior of studied orthoferrites, the magnetization (M) measurements as a function of applied magnetic field (H) have been performed at room temperature (300 K) as well as at 80 K.

Figures 8 and 9 represent the isothermal dc magnetization hysteresis (M-H) curves for $GdFe_{1-x}Ni_xO_3$ (x = 0.0, 0.1, 0.2, and 0.3) at 300 K and 80 K, respectively. It is interesting to notice that all the samples exhibit non-saturating hysteresis curves demonstrating the canted type antiferromagnetic behavior in these orthoferrites. Also an enhancement in the magnetization at 80 K has been observed as compared to that at 300 K for all the compositions, which can be attributed to the reduced thermal fluctuations of spins at lower temperature. At room temperature, the magnetization curve for $GdFeO_3$ sample is highly asymmetric, similar type of behavior has also been noticed in $PrFeO_3$ orthoferrite.[11]

The effect of Ni substitution on magnetization can be clearly seen, as the M-H curves tend to be more symmetric at room temperature (see Fig. 8). Moreover the doping affects the magnitude of magnetization differently at 300 K and 80 K. The experimental values of corecivity and retentivity at 300 K and 80 K for each sample are listed in Table II. The observed magnetization behavior is complex and it semi-empirically depends upon exchange energy associated with the magnetic moment of TM, TM-O distance, and TM-O-TM angle, etc. It can be clearly noticed from XRD patterns (see Fig. 1) that Ni doping reduces the unit cell volume, which in turn affects the bond angle and bond distances resulting in different magnetic properties as compared to pure $GdFeO_3$.

The shape of hysteresis curve at 300 K (see Fig. 8) for x = 0.1, 0.2, 0.3 samples shows that the magnetization does not saturate up to applied field and the slope $\partial M/\partial H$(taken in the linear variation of M with H) is less than that of pure specimen (x = 0.0). This indicates that AF coupling in doped samples is weaker than that of pure sample. This in turn contributes to the enhancement of retentivity in doped samples thus aligning a larger fraction of Fe^{3+} ion's magnetic moments. The decrease in magnetization at room temperature in x = 0.2, 0.3 as compared to x = 0.1 samples was

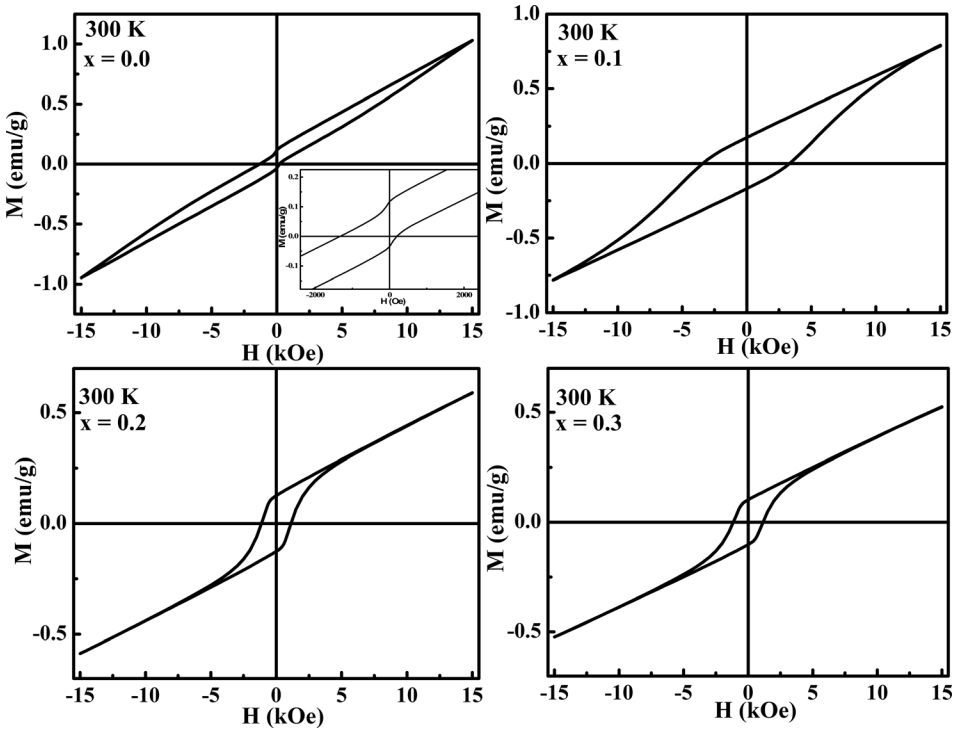

FIG. 8. Isothermal magnetization curves for x = 0.0, 0.1, 0.2, 0.3 bulk powders at 300 K.

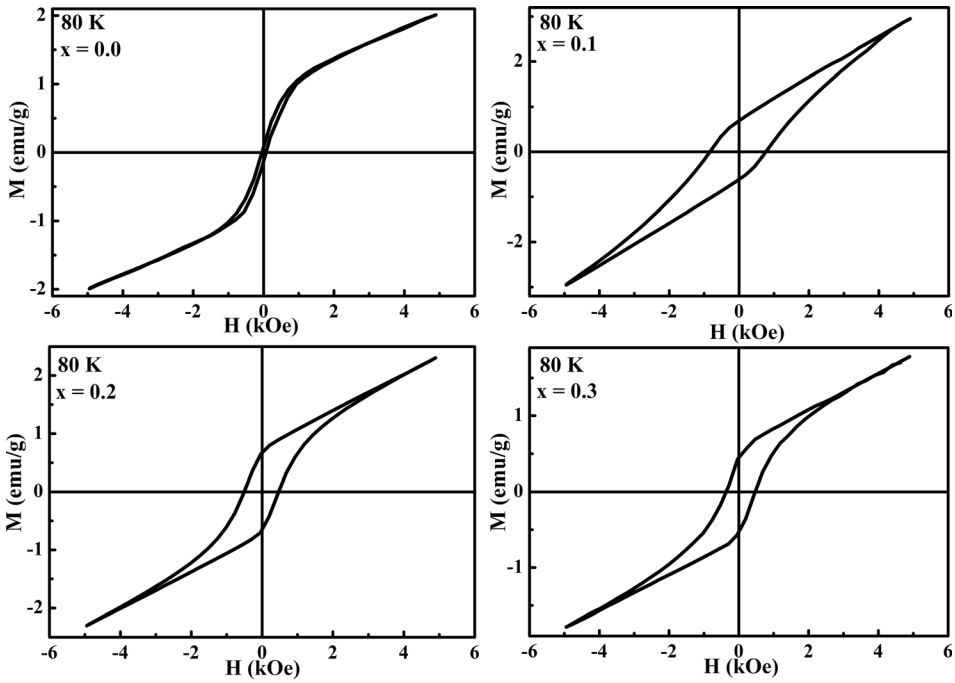

FIG. 9. Isothermal magnetization curves for all the compositions at 80 K.

TABLE II. The coercivity, retentivity, and magnetization for the reversal curve of $GdFe_{1-x}Ni_xO_3$ ($0.0 \leq x \leq 0.3$) orthoferrites at 80 K and 300 K.

	Corecivity (kOe)		Retentivity (emu/g)		Magnetization (emu/g)	
x	80 K	300 K	80 K	300 K	80 K	300 K
0.0	0.0477	1.3220	0.0786	0.1155	1.9625	1.0178
0.1	0.8235	3.3905	0.6913	0.1719	2.9643	0.7885
0.2	0.4965	1.1329	0.6739	0.1280	2.2727	0.5836
0.3	0.3576	1.1200	0.4434	0.1030	1.1740	0.5299

expected as larger magnetic moment Fe^{3+} (4 μB) ions are replaced by smaller moment Ni^{3+} (2 μB) ions. The decrease in magnetization in afore mentioned samples can also be attributed to enhanced contribution of the delocalized conduction band ($\sigma*$) formed by hybridization of Ni^{3+} e_g orbitals and 2p orbitals of O^{2-} ions.[27] Enhanced delocalization has also been supported by the dielectric measurements discussed earlier. Such type of decrease in the magnetization with Ni doping in orthoferrites has also been reported by other authors.[12,13]

Moreover, an increase in magnetization for 10% and 20% Ni^{3+} doped samples at 80 K (see Fig. 9) as compared to pure

sample can be explained on the basis of the interaction between Gd^{3+} and Ni^{3+} ions. Gilleo reported a large interaction between Gd^{3+} and Fe^{3+} ions at 75 K, this temperature is in close proximity with the considered temperature in the present study.[10] Hence, the Ni^{3+} ions incorporated in the matrix may generate different effective internal fields acting on gadolinium ions leading to different magnetic contribution from the latter.

Another reason for the observed behavior can be due to the existence of Jahn-Teller (JT) effect, as Ni^{3+} ($t_{2g}^6 e_g^1$) ions are known to induce JT distortions in $GdNiO_3$ matrix with single electron in orbitally degenerate ground state.[28] In $x = 0.1$ sample, John teller effect is small which can reduce AF coupling consequently enforcing the ferromagnetic coupling. Such type of behavior has also been noticed in $SmFe_{1-x}Mn_xO_3$ orthoferrites.[29] The decrease in the magnetization for $x = 0.3$ samples in the whole temperature range as compared to other samples can be attributed to the fact that increase in Ni^{3+} ion doping induces more free electrons as well as enhances Ni^{3+}-Ni^{3+} antiferromagnetic interactions. Moreover, the variation in the magnetic properties of $GdFe_{1-x}Ni_xO_3$ ($0.0 \leq x \leq 0.3$) orthoferrites can also be correlated to the difference in the hybridization of transition metal ion and O^{2-} ion orbitals.

It can also be noticed from the isothermal magnetization curves that the corecivity increases with increase in temperature as well as on doping. The corecivity enhancement at 300 K as compared to 80 K for all the samples can be attributed to the thermal dependence of anisotropy field and exchange field as reported by Mathur *et al.* in $YFeO_3$.[30] The observed increase in corecivity with doping can be due to change in magnetocrystalline anisotropy induced by variation in bond angles, bond lengths, and exchange energy. Similar type of corecivity enhancement in doped orthoferrites induced by variation in internal stresses has also been reported by other research groups.[29,31]

CONCLUSION

The Rietveld fitted XRD patterns confirm the formation of single phase $GdFe_{1-x}Ni_xO_3$ ($x = 0.0, 0.1, 0.2, 0.3$) orthoferrites having an orthorhombic crystal structure with Pbnm space group. The unit cell volume contraction is seen with Ni^{3+} ion substitution. Dielectric constant, tangent loss, and dielectric modulus all show a strong dependence on frequency, temperature as well as on Ni doping. Enhancement in dielectric constant, tangent loss in the doped samples at higher temperatures may be due to enhanced carrier concentration induced by Ni^{3+} ions which is further supported by decrease in activation energy. All the samples exhibit non-Debye type relaxation behavior which has been noticed from the stretched exponent ($\beta < 1$) as well as from the Cole-Cole plots. Magnetization study reveals the non-saturating hysteresis curves demonstrating the canted type antiferromagnetic behavior in these orthoferrites. Enhancement in corecivity in doped samples can be attributed to the variation in magnetocrystalline anisotropy. The variation of magnetization in $GdFe_{1-x}Ni_xO_3$ ($0.0 \leq x \leq 0.3$) orthoferrites is complex and can also be correlated to the difference in hybridization in transition metal ion and O^{2-} ion orbitals. The prepared Ni doped orthoferrites material may find its application in the decoupling capacitors. This work concludes that the Nickel doping has substantially modified the structural, dielectric and magnetic properties of $GdFeO_3$ orthoferrite.

ACKNOWLEDGMENTS

We are thankful to Dr. K. Asokan for providing the facility for low temperature dielectric measurements at the Inter University Accelerator Centre, New Delhi, India.

[1]A. Tiwari, C. Jin, and J. Narayan, Appl. Phys. Lett. **80**, 4039 (2002).
[2]L. M. Berndt, V. Balbarin, and Y. Suzuki, Appl. Phys. Lett. **77**, 2903 (2000).
[3]M. L. Moreira, E. C. Paris, G. S. Nascimento, V. M. Longo, J. R. Sambrano, V. R. Mastelaro, M. I. B. Bernardi, J. Andrés, J. A. Varelae, and E. Longo, Acta Mater. **57**, 5174 (2009).
[4]H. Forestier and G. Guilt-Guillain, C. R. Acad. Sci. **230**, 1884 (1950), available at http://gallica.bnf.fr/ark:/12148/bpt6k3182n/f1844.image.
[5]D. Treves, Phys. Rev. **125**, 1843 (1962).
[6]M. P. Pasternak, W. M. Xu, G. Kh. Rozenberg, and R. D. Taylor, Mat. Res. Soc. Symp. Proc. **718**, D2.7.1 (2002), available at http://lib-www.lanl.gov/cgi-bin/getfile?00937171.pdf.
[7]A. Wu, H. Shen, J. Xu, Z. Wang, L. Jiang, L. Luo, S. Yuan, S. Cao, and H. Zhang, Bull. Mater. Sci. **35**, 259 (2012).
[8]T. G. Ho, T. D. Ha, Q. N. Pham, H. T. Giang, T. A. T. Do, and N. T. Nguyen, Adv. Nat. Sci.: Nanosci. Nanotechnol. **2**, 015012 (2011).
[9]S. Geller, J. Chem. Phys. **24**, 1236 (1956).
[10]M. A. Gilleo, J. Chem. Phys. **24**, 1239 (1956).
[11]R. Kumar, R. J. Choudhary, M. Ikram, D. K. Shukla, S. Mollah, P. Thakur, K. H. Chae, B. Angadi, and W. K. Choi, J. Appl. Phys. **102**, 073707 (2007).
[12]R. Kumar, R. J. Choudhary, M. W. Khan, J. P. Srivastava, C. W. Bao, H. M. Tsai, J. W. Chiou, K. Asokan, and W. F. Pong, J. Appl. Phys. **97**, 093526 (2005).
[13]A. Bashir, M. Ikram, R. Kumar, P. Thakur, K. H. Chae, W. K. Choi, and V. R. Reddy, J. Phys. Condens. Matter **21**, 325501 (2009).
[14]P. Thompson, D. E. Cox, and J. B. Hastings, J. Appl. Cryst. **20**, 79 (1987).
[15]M. Idrees, M. Nadeem, and M. M. Hassan, J. Phys. D: Appl. Phys. **43**, 155401 (2010).
[16]J. C. Maxwell, *Electricity and Magnetism* (Oxford University Press, New York, 1973).
[17]C. G. Koops, Phys. Rev. **83**, 121 (1951).
[18]I. Ahmad, M. J. Akhtar, M. Younas, M. Siddique, and M. M. Hasan, J. Appl. Phys. **112**, 074105 (2012).
[19]M. Bhat, B. Kaur, R. Kumar, S. K. Khosa, K. K. Bamzai, P. N. Kotru, and B. M. Wanklyn, Nucl. Instrum. Methods Phys. Res., Sect. B **245**, 480 (2006).
[20]A. Sylvestre, S. Kukiełka, D. M. Nguyen, W. Gulbiński, and Y. Pauleau, Rev. Adv. Mater. Sci. **15**, 185 (2007), available at http://www.ipme.ru/e-journals/RAMS/no_31507/kukielka2.pdf.
[21]R. Nongjai, S. Khan, K. Asokan, H. Ahmed, and I. Khan, J. Appl. Phys. **112**, 084321 (2012).
[22]M. A. Ahmed, S. F. Mansour, and M. Afifi, J. Magn. Magn. Mater. **324**, 4 (2012).
[23]F. A. Grant, J. Appl. Phys. **29**, 76 (1958).
[24]N. H. Vasoya, V. K. Lakhani, P. U. Sharma, K. B. Modi, R. Kumar, and H. H. Joshi, J. Phys. Condens. Matter **18**, 8063 (2006).
[25]R. Pandit, K. K. Sharma, P. Kaur, R. K. Kotnala, J. Shah, and R. Kumar, J. Phys. Chem. Solids **75**, 558 (2014).
[26]S. Mathur, H. Shen, N. Lecerf, A. Kjekshus, H. Fjellvag, and G. F. Goya, Adv. Mater. **14**, 1405 (2002).
[27]M. Idrees, M. Nadeem, M. Mehmood, M. Atif, K. H. Chae, and M. M. Hassan, J. Phys. D: Appl. Phys. **44**, 105401 (2011).
[28]J. A. Alonso, M. J. Martinez-Lope, M. T. Casais, J. L. Martinez, G. Demazeau, A. Largeteau, J. L. Garcia-Munoz, A. Munoz, and M. T. Fernandez-Diaz, Chem. Mater. **11**, 2463 (1999).
[29]K. Bouziane, A. Yousif, I. A. Abdel-Latif, K. Hricovini, and C. Richter, J. Appl. Phys. **97**, 10A504 (2005).
[30]S. Mathur, M. Veith, R. Rapalaviciute, H. Shen, G. F. Goya, W. L. M. Filho, and T. S. Berquo, Chem. Mater. **16**, 1906 (2004).
[31]L. Na-Na, L. Hui, T. Rui-Lian, H. Dan-Dan, Z. Yong-Sheng, G. Wei, Z. Pin-Wen, and W. Xin, Chin. Phys. B **23**, 046105 (2014).